

## MODIFIED HALLOYSITE FOR INTESTINAL DRUG DELIVERY

Adi GHEBAUR<sup>1</sup>, Brindusa BALANUCA<sup>2</sup>, Nicoleta Mihaela FLOREA<sup>3</sup>, Aiza WATZLAVECK<sup>4</sup>, Horia IOVU<sup>5</sup>

*In this work, the modification of halloysite (HNT) with 3-methacryloxypropyltrimethoxysilane (MPTMS) was done in order to obtain a drug delivery system with reduce drug release in simulated gastric fluid. The modification of halloysite was demonstrated by FTIR, TGA and DSC. Different amounts, determined by UV-VIS, of diphenhydramine hydrochloride (DPH) were loaded within the halloysite. A comparison between the drug release profiles of DPH from pristine HNT and MPTMS modified HNT was realized and a drastic reducing in release drug amount was observed.*

**Keywords:** drug delivery, halloysite, 3-methacryloxypropyltrimethoxysilane, diphenhydramine hydrochloride

### 1. Introduction

In oral drug administration the transport of active substances at bowel level is essential for their therapeutic effect because the human intestines present a high absorption surface area [1]. The transport of drugs to liver through the intestinal barrier predicts the oral bioavailability of the active substance [2]. A drug delivery system used for the release in intestine has to protect the active substance passing through the stomach (low pH buffer solution) thus reducing to minimum the release. A large variety of delivery systems have been used until now in this matter: enteric coated drug delivery systems for which the active substance is coated with a pH sensitive polymer [3]; sustained release drug delivery systems that are time and pH dependent systems [4]; prodrug systems [5]; enzymatic degradable carriers [6]. Usually the polymers used in the synthesis of this type of drug delivery systems are natural polymers like alginate, chitosan,

<sup>1</sup> PhD, Advanced Polymer Materials Group, University POLITEHNICA of Bucharest, Romania, e-mail: ghebaudi@yahoo.com

<sup>2</sup> PhD, Advanced Polymer Materials Group, University POLITEHNICA of Bucharest, Romania, e-mail: brindusa.balanuca@yahoo.com

<sup>3</sup> PhD, Horia Hulubei – National Institute for Physics and Nuclear Engineering (IFIN-HH), Magurele, Romania, e-mail: s\_nicoleta2005us@yahoo.com

<sup>4</sup> Student, Advanced Polymer Materials Group, University POLITEHNICA of Bucharest, Romania, e-mail: aiza.watzlawek@yahoo.com

<sup>5</sup> Prof., Advanced Polymer Materials Group, University POLITEHNICA of Bucharest, Romania, e-mail: iovu@tsocm.upb.ro

locust bean gum or synthetic polymers like ethyl cellulose, hydroxypropyl methyl cellulose, Eudragites®, cellulose acetate phthalate [7].

Other types of materials intensely used in drug delivery field are clay minerals. They can be used either as excipients or they may act as transporters for the active substances being especially used in the treatment of gastrointestinal and topical diseases [8]. From all clay minerals, halloysite ( $\text{Al}_2(\text{OH})_4\text{Si}_2\text{O}_5 \text{ nH}_2\text{O}$ ) shows a high drug loading capacity due to its tubular shape, the drug being encapsulated within the lumen [9]. In order to control the drug release profile of drugs the halloysite can be modified with different types of silane coupling agents, polymers, etc. [10, 11].

The aim of this study was to synthesize a drug delivery system based on 3-methacryloxypropyltrimethoxysilane modified halloysite that reduces the released drug amount in stomach so that a higher quantity of diphenhydramine hydrochloride (DPH) may be released in intestine. The modification of halloysite with 3-methacryloxypropyltrimethoxysilane (MPTMS) was demonstrated by FTIR, TGA and DSC. The influence of initial drug concentration onto the encapsulation efficiency and the drug release profile was also determined.

## 2. Materials and Methods

### 2.1. Materials

Diphenhydramine hydrochloride was used as an active substance. 3-methacryloxypropyltrimethoxysilane the coupling agent was used to modify the clay. Toluene is the solvent employed for the silanization reaction. Halloysite (HNT) was used as a drug carrier. It has a diameter between 30 nm and 70 nm, a length of 1.3  $\mu\text{m}$ , a pore size of 1.26-1.34 mL/g, a surface area of 64  $\text{m}^2/\text{g}$  and a cation exchange capacity of 8 mequiv/100 g being purchased from Sigma-Aldrich. All materials were received from Sigma Aldrich and were used without further purification.

### 2.2. Sample preparation

The synthesis of HNT-MPTMS-DPH drug delivery systems was done in two stages according to Fig. 1. In the first stage the modification of halloysite with a silane coupling agent was achieved. 1 g of HNT was swelled in 25 mL toluene for 1 h at 80 °C then 0.9 g MPTMS amount was added. The silanization reaction was maintained at reflux under  $\text{N}_2$  atmosphere for 6 h at 100 °C. The suspension was centrifuged and washed 2 times with toluene and 3 times with water. The samples were dried under vacuum for 48 h at 60 °C and grounded to obtain a fine powder. The second stage consists in loading with DPH of modified halloysite. A precise amount of modified HNT was magnetically steered in DPH solutions of different concentrations (10 mg/mL, 40 mg/ml, 120 mg/mL, 250 mg/mL) for 1 h. The suspension was separated by centrifugation and DPH modified HNT was

dried at room temperature (RT). The resulted DPH solution was further used to determine the amount of loaded drug within HNT lumen.

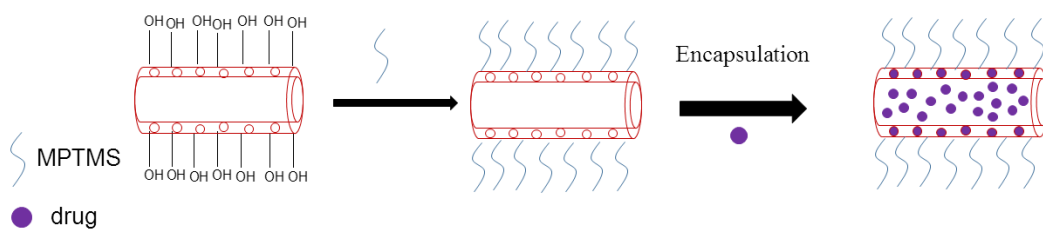


Fig. 1. The synthesis of methacrylated modified halloysite loaded with DPH

### 2.3. Methods

FTIR spectra were recorded on a Bruker VERTEX 70 spectrometer using 32 scans with a resolution of  $4\text{ cm}^{-1}$  in  $4000 - 400\text{ cm}^{-1}$  region. The samples were analyzed from KBr pellets.

Thermogravimetric analysis (TGA) was done on a Q 500 TA Instrument. The samples of 2 mg were heated from 20 to  $920\text{ }^{\circ}\text{C}$  at a scanning rate of  $10\text{ }^{\circ}\text{C}/\text{min}$  under a constant nitrogen flow rate (40 mL/min).

DSC curves were registered on a Netzsch DSC 204 F1 Phoenix equipment. The samples were heated from 20 to  $200\text{ }^{\circ}\text{C}$  using a heating rate of  $10\text{ }^{\circ}\text{C}/\text{min}$ , under a constant nitrogen flow rate (40 mL/min).

UV-Visible absorbance of VB<sub>1</sub> solutions was measured at  $\lambda_{\text{max}} = 259\text{ nm}$  (Cary 60 Agilent equipment) provided with a quartz cell having a light path of 10 mm.

The drug release profile was determined in an automated dissolution USP Apparatus 1 (708-DS Agilent) with an selfcontrolled multi-channel peristaltic pump (810 Agilent), an UV/VIS spectrophotometer (Cary 60) with 1 mm flow cell and UV-Dissolution software. The samples were put in a dialysis membrane with 5 mL simulated fluid, attached by the dissolution bath rod and immersed in 200 mL of dissolution medium at  $37\text{ }^{\circ}\text{C}$ . Rotational speed of 75 rpm was tested. The samples were maintained for 24 h in simulated gastric fluid/simulated intestinal fluid without enzymes (SGF/SIF) and at specific time intervals the amount of released DPH was determined with a known concentration of the standard solutions at 259 nm wavelength. SGF (pH 1.2) consists of 2 g sodium chloride dissolved in 7 mL of hydrochloric acid (420 g/L) and sufficient water to produce 1000 mL solution. SIF (pH 6.8) contains 77 mL of sodium hydroxide (0.2 mol/L) and 6.8 g potassium dihydrogen phosphate and sufficient water to produce 1000 mL solution.

### 3. Results and discussion

#### 3.1. Characterization of MPTMS modified HNT

##### 3.1.1. FTIR analysis

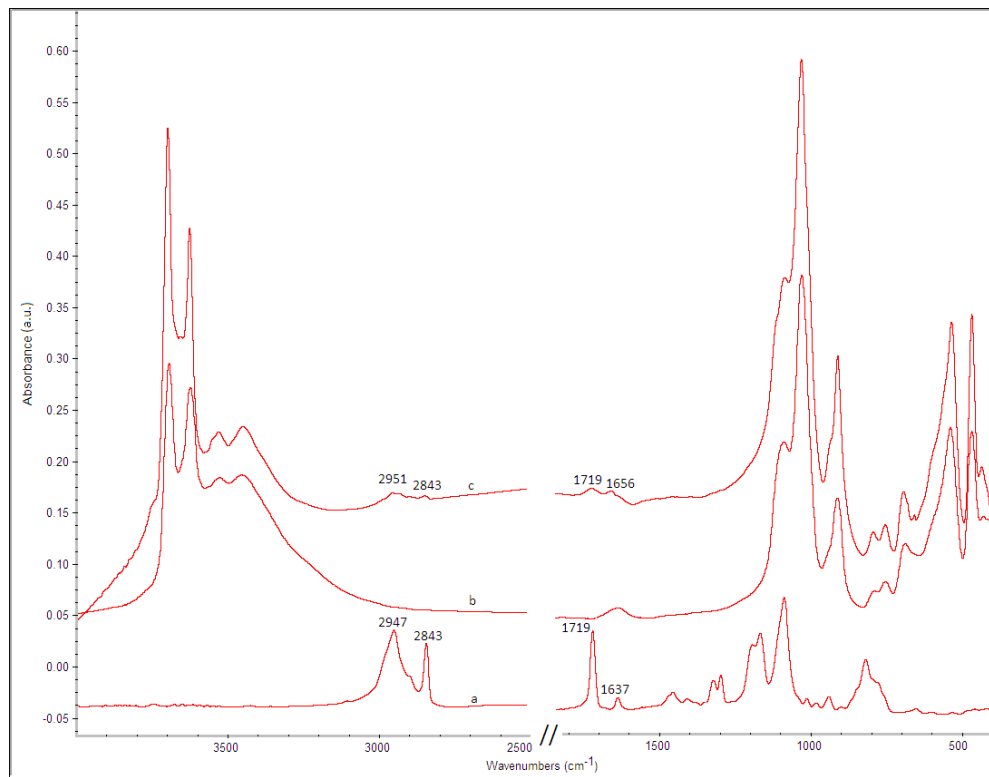


Fig. 2. FTIR spectra of: a) MPTMS; b) HNT; c) HNT-MPTMS

A preliminary technique employed to demonstrate the modification of HNT with MPTMS was FTIR. In Fig. 2 the FTIR spectra for MPTMS, HNT and HNT-MPTMS are shown. The absorption peaks from MPTMS at  $2947\text{ cm}^{-1}$  and  $2843\text{ cm}^{-1}$  are attributed to the asymmetric stretching vibration of C-H bond from  $\text{CH}_3$  group, respectively to the symmetric stretching vibration of C-H bond from  $\text{O-CH}_2$ . The peaks characteristic to methacrylic groups are present at  $1719\text{ cm}^{-1}$  associated to the stretching vibration of  $\text{C=O}$  bond and at  $1637\text{ cm}^{-1}$  assigned to the stretching vibration of  $\text{C=C}$  bond [12,13]. The same peaks may also be observed in HNT-MPTMS spectrum at  $2951\text{ cm}^{-1}$  ( $\nu_{\text{as}}$  C-H),  $2843\text{ cm}^{-1}$  ( $\nu_{\text{s}}$  C-H),  $1719\text{ cm}^{-1}$  ( $\nu$  C=O) and  $1656\text{ cm}^{-1}$  ( $\nu$  C-O). This is a proof that the silanization of HNT took place and methacryl groups were grafted on its surface.

### 3.1.2. Thermogravimetric analysis

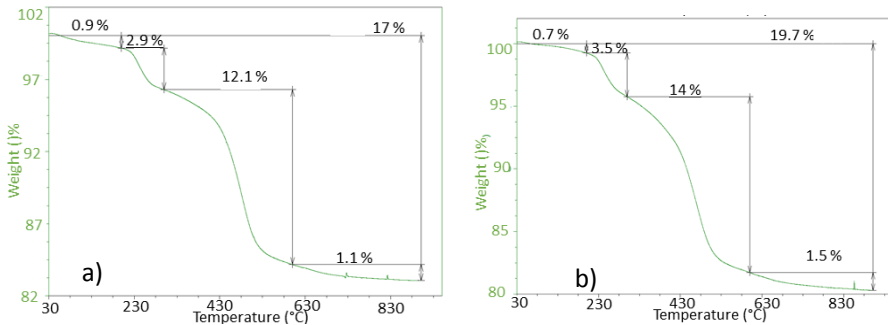


Fig. 3. TGA curves of pure HNT (a) and HNT-MPTMS b)

The thermogravimetric curves of pure HNT and HNT modified with MPTMS are shown in Fig. 3. The both unmodified and modified halloysite show several steps of degradation. In the first step (30-200 °C) the halloysite losses the free surface water. Unmodified halloysite has a higher weight loss (0.87 %) than HNT-MPTMS (0.74 %) because modification with MPTMS induces a hydrophobic effect to HNT [14]. The second weight loss stage (200-300 °C) is assigned to the silane groups that are bonded by the secondary interactions or they may be grafted onto HNT surface forming Si-O-Si bonds [15]. The third mass loss stage (300-600 °C) corresponds to the dehydroxylation of Al-OH and Si-OH groups of HNT. An increase of 2 wt.% of mass loss in this stage is observed in HNT-MPTMS case due to the decomposition of the organic compound from MPTMS.

### 3.1.3. Differential scanning calorimetry analysis

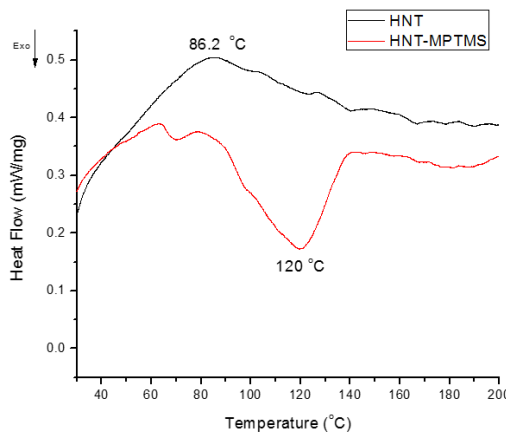


Fig. 4. DSC curves of unmodified and modified HNT

In Fig. 4 the DSC curves of unmodified and modified HNT are shown. In order to demonstrate the modification of HNT with MPTMS by DSC the HNT-MPTMS sample was mixed with 2% AIBN. The presence of the exothermic peak at 120 °C characteristic to the polymerization of methacrylic groups is another proof that the modification of HNT with MPTMS was realized. A weak endothermic peak can be observed at 86.2 °C that is also present in the HNT curve and it is attributed to the evaporation of adsorbed water [16].

### 3.2. HNT-MPTMS-SPH characterization

#### 3.2.1. FTIR analysis

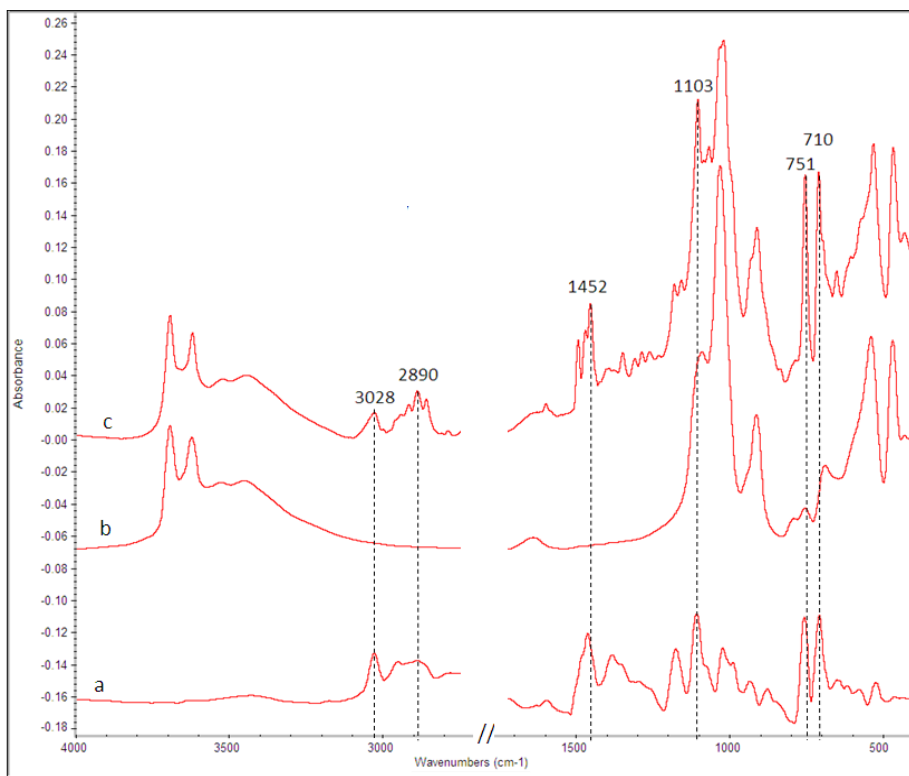


Fig. 5. FTIR spectra of a) DPH; b) HNT; c) HNT-DPH

The modification of HNT with DPH can be also demonstrated by the appearance of some characteristic peaks of drug into HNT-DPH spectrum (Fig. 5): at 3028  $\text{cm}^{-1}$  attributed to the stretching vibration of C-H bond from aryl groups and at 2890  $\text{cm}^{-1}$  assigned to the stretching vibration of C-H bond from alkyl group. Also, some small shifts were observed in the HNT-DPH spectrum for the next peaks: from 1461  $\text{cm}^{-1}$  to 1452  $\text{cm}^{-1}$ , attributed to C-N<sup>+</sup> bond and for the

peaks assigned to the C-H out of plane bending vibrations of mono substituted phenyl from  $710\text{ cm}^{-1}$  to  $704\text{ cm}^{-1}$  and from  $751\text{ cm}^{-1}$  to  $755\text{ cm}^{-1}$  [17]. In the spectrum of HNT-MPTMS-DPH (Fig. 6) the presence of a peak at  $3023\text{ cm}^{-1}$  attributed to the stretching vibration of C-H bond and the peak at  $1457\text{ cm}^{-1}$  assigned to C-N<sup>+</sup> bond were observed.

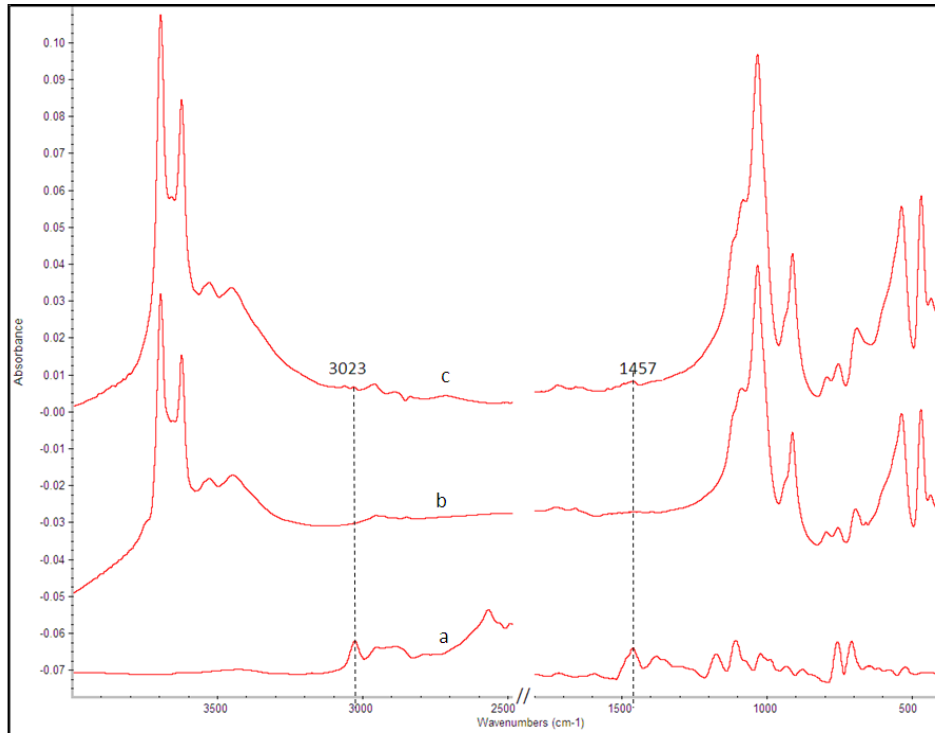


Fig. 6. FTIR spectra of a) DPH; b) HNT-MPTMS; c) HNT-MPTMS-DPH

### 3.2.2. Encapsulation efficiency

The influence of initial drug concentration on the encapsulation efficiency process of DPH onto HNT was studied. The encapsulation efficiency (EE %) was calculated using equation (1):

(1)

where  $m_0$  is the initial drug amount (g),  $m$  is the unloaded drug amount (g).

As can be observed from Table 1 if a higher amount of drug is used at the loading process the EE % increases and in the case of modified HNT the entire

amount of drug is encapsulated. This may be due to the modification of the surface area created by modification with MPTMS [18].

**Table 1**  
**The influence of initial drug concentration onto encapsulation efficiency**

Sample, mg/mL	EE [%]
HNT-DPH 10	81
HNT-DPH 40	88.3
HNT-DPH 120	89.6
HNT-DPH 250	89.7
HNT-MPTMS-DPH 10	96.3
HNT-MPTMS-DPH 40	98.2
HNT-MPTMS-DPH 120	99.9
HNT-MPTMS-DPH 250	99.6

### 3.2.3. *In vitro* drug release

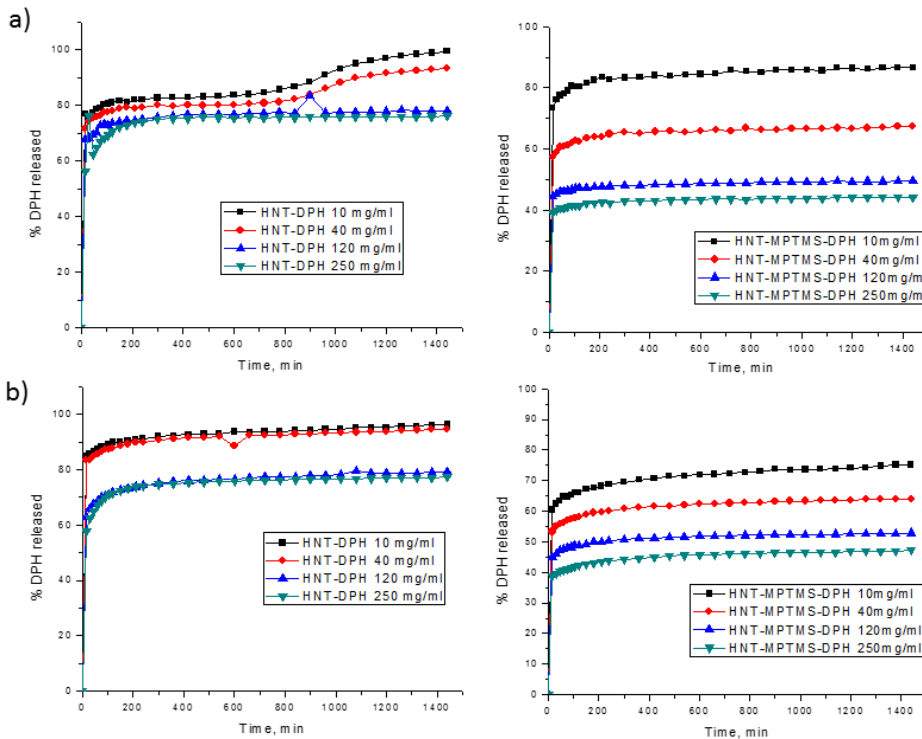


Fig. 6. Drug release profile of DPH in SIF (a) and SGF (b) from unmodified and modified HNT

The *in vitro* drug release of unmodified HNT and MPTMS modified HNT doped with DPH was studied in SGF and SIF. As can be observed in Fig. 7 a high concentration of drug is released from the samples that contain the lowest amount

of active substance while for the systems with the highest loaded drug amount the release profile presents the lowest concentration. This phenomenon takes place in both SGF and SIF. If the release profile of DPH from HNT is compared to that of HNT-MPTMS one may conclude that the methacrylate group attached on HNT surface reduces the release amount of drug with around 20 %.

#### 4. Conclusions

In this study, new drug delivery systems based on modified MPTMS halloysite with reduced drug release in low pH buffer solution were synthesized. The modification of HNT with MPTMS was demonstrated by different characterization techniques like FTIR through the presence of different peaks characteristic to methacrylic groups, TGA where a higher final weight loss was registered for the modified clay due to the degradation of the coupling agent and through DSC by the appearance of an exothermic peak from the polymerization of methacrylic groups that are attached on HNT surface. The influence of the initial drug concentration within HNT lumen was also studied and it was observed that the higher the amount of drug added, higher encapsulation efficiency was registered especially in HNT-MPTMS case. The *in vitro* drug release indicates that the modification of HNT with MPTMS reduces significantly the release amount of DPH in simulated gastric fluid (SGF).

#### Acknowledgement

The work has been funded by the Sectoral Operational Programme Human Resources Development 2007-2013 of the Ministry of European Funds through the Financial Agreement POSDRU/159/1.5/S/132397.

#### R E F E R E N C E S

- [1]. *K.S. Pang*, “Modeling of intestinal drug adsorption: Roles of transporters and metabolic enzymes (for the Gillette review series)”, in *Drug Metab. Dispos.*, **vol. 31**, no. 12, Dec. 2003, pp. 1507-1519
- [2]. *N.L. Trevisakis, W.N. Charman, C.J.H. Porter*, “Lipid based systems and intestinal lymphatic drug transport: A mechanistic update”, in *Adv. Drug Deliver. Rev.*, **vol. 60**, no. 6, March 2008, pp. 702-716
- [3]. *M. Rodríguez, J.L. Vila-Jato, D. Torres*, “Design of a new multiparticulate system for potential site-specific and controlled drug delivery to the colonic region”, *J. Control. Release*, **vol. 55**, no. 1, Oct. 1998, pp. 67-77
- [4]. *L. Zema, A. Maroni, A. Foppoli, L. Palugan, M.E. Sangalli, A. Gazzaniga*, “Different HPMC viscosity grades as coating agents for an oral time and/or site-controlled delivery system: an investigation into the mechanisms governing drug release”, *J. Pharm. Sci.*, **vol. 96**, no. 6, Jun. 2007, pp. 1527-1536
- [5]. *D.R. Friend*, “New oral delivery systems for treatment of inflammatory bowel disease”, *Adv. Drug Deliv. Rev.*, **vol. 57**, no. 2, Jan. 2005, pp. 247-265

- [6]. *F. Talaei, E. Azizi, R. Dinarvand, F. Atyabi*, “Thiolated chitosan nanoparticles as a delivery system for antisense therapy: evaluation against EGFR in T47D breast cancer cells”, *Int. J. Nanomed.*, **vol. 6**, Sept. 2011, pp. 1963–1975
- [7]. *F. Talaei, F. Atyabi, M. Azhdarzadeh, R. Dinarvand, A. Saadatzadeh*, “Overcoming therapeutic obstacles in inflammatory bowel diseases: A comprehensive review on novel drug delivery strategies”, *Eur. J. Pharm Sci.*, **vol. 49**, no. 4, Jul. 2013, pp. 712–722
- [8]. *C. Viseras, P. Cerezo, R. Sanchez, I. Salcedo, C. Aguzzi*, “Current challenges in clay minerals for drug delivery”, *Appl. Clay Sci.*, **vol. 48**, no. 3, Apr. 2010, pp. 291-295
- [9]. *Q. Wang, J. Zhang, Y. Zheng, A. Wang*, “Adsorption and release of ofloxacin from acid- and heat-treated halloysite”, *Colloid. Surface. B.*, **vol. 113**, Jan. 2014, pp. 51-58
- [10]. *D. Tan, P. Yuan, F. Annabi-Bergaya, D. Liu, L. Wang, H. Liu, H. He*, “Loading and *in vitro* release of ibuprofen in tubular halloysite”, *Appl. Clay Sci.*, **vol. 96**, Jul. 2014, pp. 50-55
- [11]. *G. Cavallaro, G. Lazzara, M. Massaro, S. Milioto, R. Noto, F. Parisi, S. Riela*, “Biocompatible Poly(N-isopropylacrylamide)-halloysite Nanotubes for Thermoresponsive Curcumin Release”, *J. PHYS. Chem. C.*, **vol. 119**, no. 16, 2015, pp. 8944-8951
- [12]. *M. Masmoudi, M. Abdelmouleh, R. Abdelhedi*, “Infrared characterization and electrochemical study of  $\gamma$ -methacryloxypropyltrimethoxysilane grafted in to surface of cooper”, *Spectrochim. Acta A*, **vol. 118**, 2014, pp. 643-650
- [13]. *J. Zhang, Z. Guo, X. Zhi, H. Tang*, “Surface modification of ultrafine precipitated silica with 3- methacryloxypropyltrimethoxysilane in carbonization process”, *Colloid. Surface. A.*, **vol. 418**, Feb. 2013, pp. 174-179
- [14]. *M.U. de la Orden, J. Arranz, V. Lorenzo, E. Pérez, J. Martínez Urreaga*, “Study of the effects of the reaction conditions on the modification of clays with polyelectrolytes and silanes”, *J. Colloid. Interf. Sci.*, **vol. 342**, no. 1, Feb 2010, pp. 185-191
- [15]. *L.N. Carli, T. S. Daitx, G.V. Soares, J. S. Crespo, R.S. Mauler*, “The effect of silane coupling agents on the properties of PHBV/halloysite nanocomposites”, *Appl. Clay Sci.*, **vol. 87**, Jan. 2014, pp. 311-319
- [16]. *H. Lun, J. Ouyang, H. Yang*, “Natural halloysite nanotubes modified as an aspirin carrier”, *RCS Adv.*, **vol. 4**, no. 83, Sept. 2014, pp. 44197-44202
- [17]. *S.T. Ulu, F.T. Elmali*, “Spectrophotometric method for the determination, validation, spectroscopic and thermal analysis of diphenhydramine in pharmaceutical preparation”, *Spectrochim. Acta A.*, **vol. 77**, no. 1, Sept. 2010, pp. 324-329
- [18]. *Y.-F. Shi, Z. Tian, Y. Zhang, H.-B. Shen, N.-Q. Jia*, “Functionalized halloysite nanotube-based carrier for intracellular delivery of antisense oligonucleotides”, *Nanoscale Res. Lett.*, **vol. 6**, no. 608, 2011, pp. 1-7